Electronic Supplementary Material (ESI) for ChemComm.

Electronic Supplementary Information

Strong ^{31}P nuclear spin hyperpolarization produced via reversible chemical interaction with parahydrogen

Vladimir V. Zhivonitko,*[†] Ivan V. Skovpin[†] and Igor V. Koptyug[†,‡]

[†]Laboratory of Magnetic Resonance Microimaging, International Tomography Center SB RAS, Instututskaya St. 3A, 630090 Novosibirsk, Russia; [‡]Novosibirsk State University, Pirogova St. 2, 630090 Novosibirsk, Russia;

-CONTENTS-

1 Materials and Experimental Methods

1.1 General information

NMR experiments were performed on a 300 MHz Bruker AV 300 NMR spectrometer equipped with a broad-band 10 mm RF probe. The standard temperature control unit of the NMR spectrometer was used for heating the samples. Spectra detected using a single 90-degree pulse.

NMR imaging experiments were performed on a 400 MHz Bruker AV 400 NMR spectrometer equipped with microimaging accessories. A single shot fast multiple spin-echo pulse sequence was used in the imaging experiments. The numbers of points in read and phase directions were 256 and 16, respectively. The field of view was 25 by 25 mm^2. The echo time was 7 ms.

High-purity commercially available H_2 gas was used for producing parahydrogen-enriched H_2 referred in the main text as "pH_2". The enrichment was performed using Bruker parahydrogen generator (BPHG 90) which provides H_2 gas with ca. 92.3% content of parahydrogen. In the typical enrichment, H_2 from a gas cylinder was supplied to the generator, and the necessary procedures (cooling, passing through conversion catalyst) required for the enrichment the generator performed automatically. The gas from the generator outlet was collected in a small gas cylinder to be used in the experiments.

1.2 Experimental details

In a typical workflow, $(PPh_3)_3Ir(H_2)Cl$ compound was produced firstly by bubbling H_2 through toluene (normal or deuterated) solution of $[Ir_2Cl_2(COD)_2]$ and PPh_3 in a 10 mm sample (Wilmad) tubing at ca. 60˚C. As the solution became colorless, the bubbling and the heating were stopped. The resulting $(PPh_3)_3Ir(H_2)Cl$ solution was used in the experiments. Typically, the sample tube with the solution was heated up using the NMR instrument heating system to a required temperature. Thereafter it was taken out of the magnet and placed into a magnetic field shield made of μ-metal, which provided magnetic field attenuation to ca. 1 μT, and pH_2 was supplied to the bottom of the sample tube through a 1/16" PTFE tubing for 3 s. Then, the gas flow was stopped and the sample was transferred to the NMR magnet manually within ca. 1 s. The NMR spectra (^{31}P or ^{1}H) were acquired immediately after that. The concentrations of $(PPh_3)_3Ir(H_2)Cl$ and free PPh_3 in solution were about the same in all experiments (6 and 12 mM, respectively).

1.2.1 EXSY experiments

EXSY spectroscopy provided the kinetic data on the magnetization exchange rates between free PPh_3 and *trans*-PPh_3 ligand in $(PPh_3)_3Ir(H_2)Cl$ as well as between H_2 in solution and hydride

ligands in $(PPh_3)_3Ir(H_2)Cl$. For example, the kinetic curve for the equilibrium at 60˚C is shown in Figure S1.

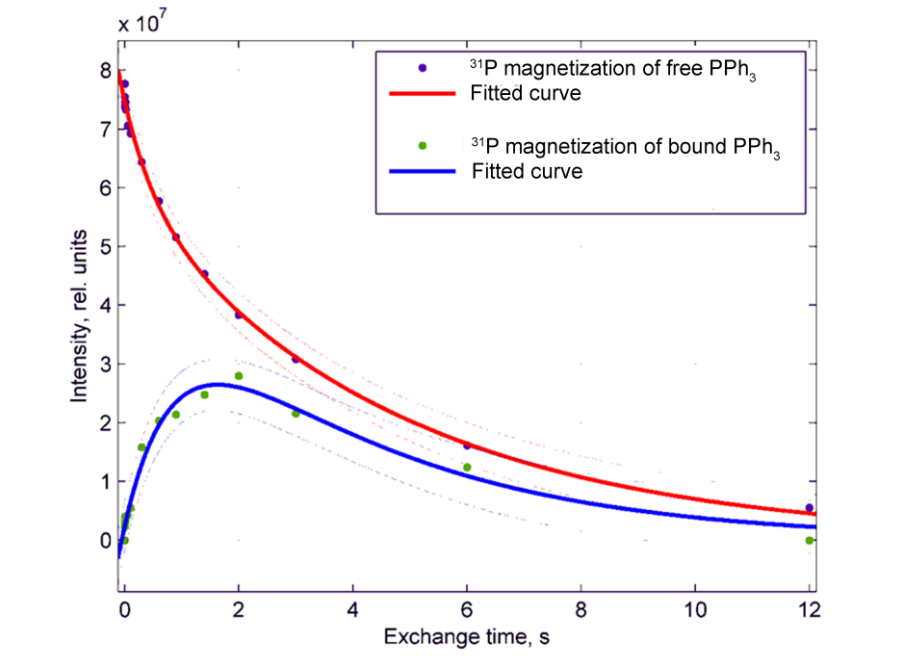

Figure S1. The kinetic curve corresponding to chemical exchange process between free PPh_3 and $(PPh_3)_3Ir(H_2)Cl$ as obtained from EXSY data at 60˚C.

The fitting analysis of kinetic data provided the exchange rate as well as the averaged relaxation rate ($1/T_1$) of the magnetization. The parameters resulting from the analysis are presented in Table 1 of the main text.

1.2.2 Simulations of ^{31}P hyperpolarization

Simulations were performed by assuming the presence of chemical exchange between *trans*-PPh_3 in $(PPh_3)_3Ir(H_2)Cl$ complex and free PPh_3 as well as between hydride ligands and pH_2. We considered the saturation of solution with pH_2 to be fast and efficient process under the bubbling conditions used in the work. The presence of benzene ring protons in PPh_3 was ignored for the sake of simplification. In the case of non-zero exchange rates, the singlet spin order of pH_2 ($E/4 - I_1 \cdot I_2$) was taken as the initial recoverable state, and the spins in the complex were considered as totally disordered. The ongoing chemical exchange brought the singlet spin order into the complex naturally during the time evolution. The experimentally measured magnetic field variation profile as a function of time during sample transfer was used in the simulations, see Figure S2. The evolution of the spin system at a required initial magnetic field followed by the sample transfer to the high magnetic field was simulated numerically by propagating density operator in the presence of chemical shift interaction, J-coupling and the chemical exchange. The single spin orders were set to

be preserved under the chemical exchange (depletion and creation processes balanced), whereas multi spin orders were set to only deplete under the exchange as the underlying chemistry presumes that the probability of same spins encounter on a reasonable time scale is very low. In the case of exchange constants set to zero (blue curve in Figure 3 of the main text), the initial state was set so that the proton pair in the complex was in the singlet state, assuming that the pair was generated due to an instant and irreversible interaction of Ir center with pH_2. The following set of spin system parameters was used in the calculations:[S1,S2] δ_1 = –10.8, δ_2 = –20.8, δ_3 = 5.7, δ_4 =5.7, δ_5 = –2.8 and δ_6 = –5.3 ppm; J_{12} = - 7, J_{13} = 20.6, J_{14} = 20.6, J_{15} = 130.6, J_{23} = 14.3, J_{24} = 14.3, J_{25} = 14.3, J_{34} = 0, J_{35} =26 and J_{45} = 26 Hz; where 1 is *trans*-H, 2 is *cis*-H, 3 is *cis*-P, 4 is another *cis*-P, 5 is *trans*-P in the complex and 6 is the free P.

The field dependencies presented in Figure 3 of the main text were calculated by varying the initial magnetic field. For example, simulated spectra corresponding to the chemical equilibrium parameters at 60 and 80˚C are shown Figure S3a and Figure S3b (initial field ca. 1 μT), respectively. Note that the nuclear spin relaxation was not included into the simulations, and the exact shape of signals may thus slightly vary due to the presence of cross-polarization effects. Generally, the simulation reproduced the features of the observed effects.

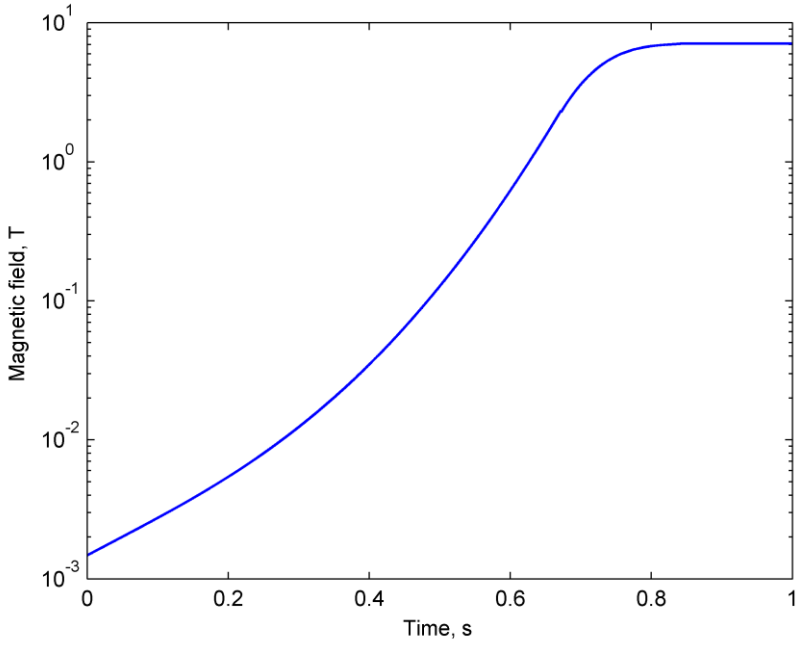

Figure S2. Experimentally measured magnetic field lifting profile on the way from the outside of the 7 T NMR magnet to the inside. Note, the first point of the initial magnetic field (in the magnetic field shield) is not shown in this graph.

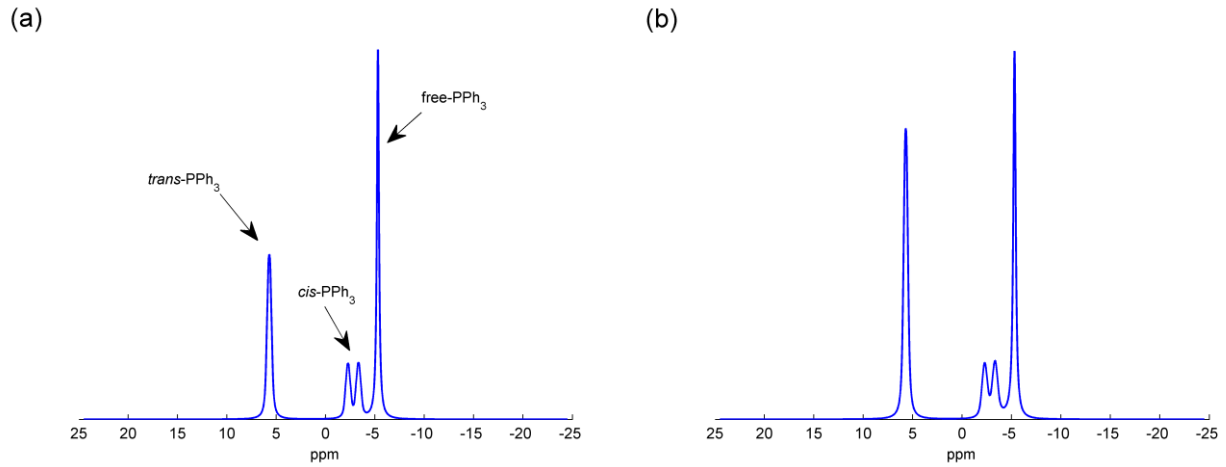

Figure S3. Simulated ^{31}P NMR spectra obtained assuming the chemical exchange between *trans*-PPh_3 in $(PPh_3)_3Ir(H_2)Cl$ and free PPh_3 and hydride lignads and pH_2 at (a) 60 and (b) 80˚C. The vertical scales for the two spectra are different.

1.2.3 2D HMBC experiments for the polarized ^1H NMR signals assignment

^1H HMBC spectrum of $(PPh_3)_3Ir(H_2)Cl$ and PPh_3 solution is shown in Figure S4. The region of benzene proton signals is shown in the figure. The obtained cross-peaks correspond to protons of PPh_3 molecules in *ortho* and *meta* positions of benzene rings of bound PPh_3 in the complex as well as free PPh_3.

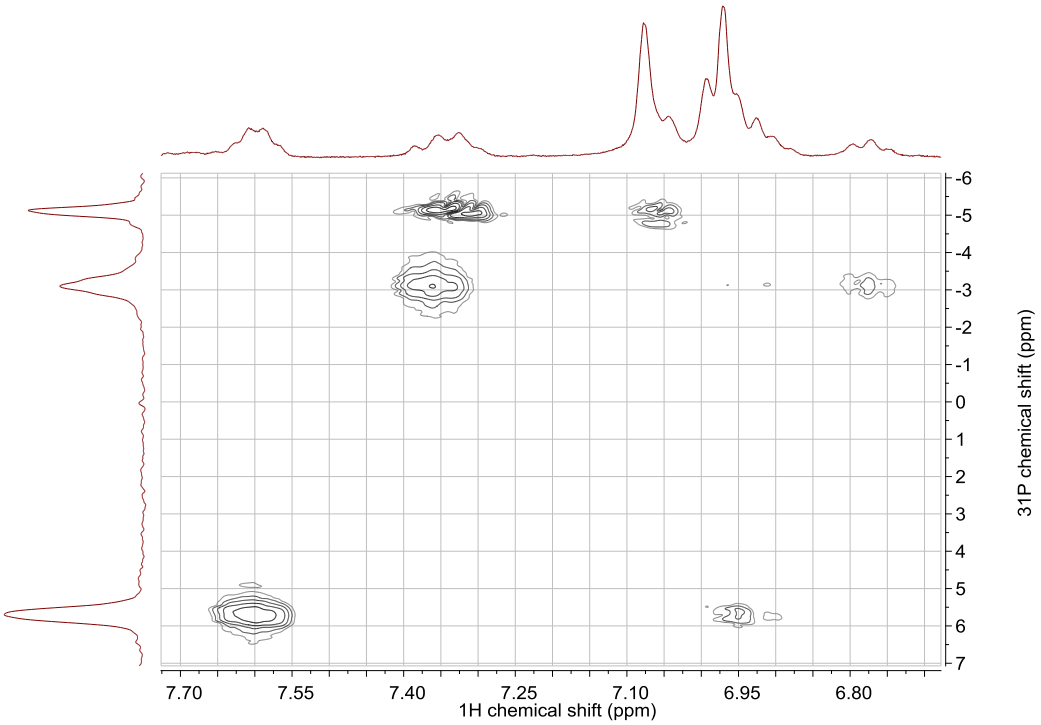

Figure S4. 2D HMBC spectrum of $(PPh_3)_3Ir(H_2)Cl$ and PPh_3 solution.

2 References

(S1) Sleigh, C. J.; Duckett, S. B.; Messerle, B. A. *Chem. Commun.* **1996**, 2395.

(S2) Messerle, B. A.; Sleigh, C. J.; Partridge, M. G.; Duckett, S. B. *J. Chem. Soc., Dalton Trans.* **1999**, 1429.